# Structure of 2,3-Butanedione Dihydrazone and IR Study of Higher Polyazines: A New Class of Polymeric Conductors

**Charles R. Hauer,[†] Gregory S. King,[†] Erica L. McCool,[†] William B. Euler,*[†] Joseph D. Ferrara,[‡] and Wiley J. Youngs*[‡]**

*Contribution from the Department of Chemistry, University of Rhode Island, Kingston, Rhode Island 02881, and the Department of Chemistry, Case Western Reserve University, Cleveland, Ohio 44106.* *Received February 24, 1987*

**Abstract:** Polyazines, $H_2N-[N=C(CH_3)-C(CH_3)=N]_x-NH_2$, of various chain lengths have been prepared and studied by IR spectroscopy. An X-ray crystal structure was done on the monomer of this series, 2,3-butanedione dihydrazone ($x = 1$). It crystallized in space group $P4_2/n$ with cell constants $a = 12.172$ (3) Å and $c = 4.115$ (1) Å and $Z = 4$; intensity data were collected from $3.0° \leq 2\theta \leq 65.0°$. Refinement to convergence on the 1195 independent reflections, $I \geq 3\sigma(I)$, resulted in final anisotropic $R = 0.043$ and $R_w = 0.048$. The monomer is planar with long carbon–nitrogen double bonds (1.291 (1) Å) in the *E* conformation, the methyl groups are anti across the short carbon–carbon single bond (1.474 (2) Å), and the lone pairs across the nitrogen–nitrogen single bonds are gauche. The anomalous bond lengths indicate a degree of $\pi$-bond conjugation in this molecule. The higher molecular weight materials are yellow to brown powders, are stable to air, have high melting points, and are surprisingly resistant to hydrolysis. Correlation of the IR spectra of the monomer and sequentially increasing chain length polymers shows that the highest molecular weight material is at least 45 monomer units long and is planar with double bonds in the *E* conformation and all single bonds in the anti conformation. As in the monomer, the position of the C=N resonance indicates conjugation of the $\pi$ system along the polymer chain. The polymer can be doped with iodine to give air-stable electrically conducting materials with room-temperature conductivities as high as 1.3 $\Omega^{-1}$ cm$^{-1}$. IR spectra of the doped materials show that the polymer retains its structural integrity, and two new doping-induced absorptions appear.

The study of polymers with extended $\pi$ systems that can be doped into electrically conducting states has been of great interest recently.[1] One such class of materials is the polyazines, $-[N=C(R)-C(R)=N]_x-$, which are formally isoelectronic with the heavily studied polyacetylene,[1a,b,2] $-[CH=CH-CH=CH]_x-$. The bond alternation opens a gap in the $\pi$ band structure in *trans*-polyacetylene; however, the $\pi$ system is said to be degenerate because a one-bond shift of the $\pi$ bond along the chain gives a structurally identical polymer. This electronic structure gives rise to the possibility of soliton midgap states that are important for understanding the physical properties of *trans*-polyacetylene.[1,2] The $\pi$ structure of polyazine is not degenerate: polyazine is the head-to-head polymer of methenimine; a one-bond shift of the $\pi$ bond along the chain would give a material with alternating azene and ethylene moieties, which is not isoenergetic with polyazine. Thus, unlike polyacetylene, polyazine cannot have soliton-like midgap states, but polaron or bipolaron states are more reasonable possibilities.[3,4]

Earlier calculations on polyazine[3] indicated that the $\pi$ band structure is somewhat different from that of polyacetylene: symmetry dictates that polyazine must have four $\pi$ bands while polyacetylene only has two and the band gap in polyazine is about twice that found in polyacetylene. Nonetheless, it was expected that oxidative doping could produce a conducting state in polyazine.

In this paper we report the preparation and IR spectra for a series of polyazines, $H_2N-[N=C(CH_3)-C(CH_3)=N]_x-NH_2$, for $x = 1$ to $x > 45$. We also report the X-ray crystal structure of the monomeric 2,3-butanedione dihydrazone ($x = 1$) and use this structure in conjunction with IR spectra of a series of polyazines to deduce the structure of the long-chain polymers. Finally, we report the results of our initial doping experiments, where materials with high room-temperature conductivities are found.

## Experimental Section

2,3-Butanedione and hydrazine hydrate were purchased from Aldrich and used as received. Solvents were reagent grade and, unless otherwise noted, were used as received. Melting points were recorded on a Mel-Temp apparatus and are uncorrected. All elemental analyses were performed by M-H-W Laboratories, Phoenix, AZ.

**$C_4H_{10}N_4$ (2,3-Butanedione Dihydrazone).** A modification of the procedure of Busch and Bailar[5] was used to prepare this compound. A solution of 30.0 mL (0.617 mol) of $NH_2NH_2{\cdot}H_2O$ and 5 drops of glacial acetic acid in 300 mL of ethanol was prepared. A solution of 12.0 mL (0.137 mol) of 2,3-butanedione dissolved in 25 mL of ethanol was added dropwise to the stirred, room-temperature hydrazine solution over the course of an hour. The resultant solution was stirred at room temperature for another 2 h, stoppered, and refrigerated overnight. Long white crystals were filtered, washed with cold ethanol, and dried under vacuum: yield, 11.88 g (0.104 mol), 76%; mp 159–160 °C, in agreement with the literature.[5a] Anal. Calcd for $C_4H_{10}N_4$: C, 42.09; H, 8.83; N, 49.08. Found: C, 42.13; H, 8.95; N, 49.11.

**$C_8H_{16}N_6$.** The procedure of Stratton and Busch[6] was followed. A solution of 25.0 mL (0.285 mol) of 2,3-butanedione in 15 mL of water was cooled to 0 °C. To this was added 6.6 mL (0.14 mol) of $NH_2NH_2{\cdot}H_2O$ dropwise over the course of 15 min. This solution was then added to 250 mL of $H_2O$ and refrigerated overnight. White crystals of biacetyl azine were filtered and washed with cold $H_2O$: yield, 14.75 g ($C_8H_{12}N_2O_2$, 0.0877 mol), 64%; mp 32–35 °C, in agreement with the literature.[6] A solution of 16.0 mL (0.329 mol) of $NH_2NH_2{\cdot}H_2O$ in 35 mL of $H_2O$ was stirred at room temperature. To this was added dropwise (30 min) a solution of 6.75 g (0.040 mol) of biacetyl azine dissolved in 20 mL of ethanol. The resultant solution was refrigerated overnight. The yellow powder was filtered and recrystallized from 50 mL of hot absolute ethanol, giving yellow microcrystals: yield, 3.65 g (0.0186 mol), 46%; mp 146–158 °C with decomposition, higher than reported by Stratton

---

[†] University of Rhode Island.

[‡] Case Western Reserve University.

(1) (a) Su, W. P.; Schrieffer, J. R.; Heeger, A. J. *Phys. Rev. Lett.* **1979**, *42*, 1698–1701. (b) Park, Y. W.; Heeger, A. J.; Druy, M. A.; MacDiarmid, A. G. *J. Chem. Phys.* **1980**, *73*, 946–957. (c) Diaz, A. F.; Kanazawa, K. K. In *Extended Linear Chain Compounds*: Miller, J. S., Ed.; Plenum: New York, 1983; Vol. 3, pp 417–441. (d) Pfluger, P.; Gubler, U. M.; Street, G. B. *Solid State Commun.* **1984**, *49*, 911–915. (e) Conwell, E. M. *Synth. Met.* **1985**, *11*, 21–28.

(2) (a) Weinberger, B. R.; Ehrenfreund, E.; Pron, A.; Heeger, A. J.; MacDiarmid, A. G. *J. Chem. Phys.* **1980**, *72*, 4749–4755. (b) Zannoni, G.; Zerbi, G. *Solid State Commun.* **1983**, *48*, 871–874. (c) Chien, J. C. W.; Karasz, F. E.; Schen, M. A.; Hirsch, J. A. *Macromolecules* **1983**, *16*, 1694–1697. (d) Thomann, H.; Dalton, L. R.; Grabowski, M.; Clarke, T. C. *Phys. Rev. B* **1985**, *31*, 3141–3143. (e) Cline, J. F.; Thomann, H.; Kim, H.; Morrobel-Sosa, A.; Dalton, L. R.; Hoffman, B. M. *Phys. Rev. B* **1985**, *31*, 1605–1607.

(3) Euler, W. B.; Hauer, C. R. *Solid State Commun.* **1984**, *51*, 473–476.

(4) (a) Bredas, J. L.; Street, G. B. *Acc. Chem. Res.* **1985**, *18*, 309–315. (b) Bredas, J. L.; Scott, J. C.; Yakushi, K.; Street, G. B. *Phys. Rev. B* **1984**, *30*, 1023–1025.

(5) (a) Busch, D. H.; Bailar, J. C. *J. Am. Chem. Soc.* **1956**, *78*, 1137–1142. (b) Hauer, C. R. Master's Thesis, University of Rhode Island, 1985.

0002-7863/87/1509-5760$01.50/0

**Table I.** Results of the $I_2$ Doping of $(C_4H_6N_2)_x$

| mass of $I_2$ reacted,[a] mg | % I in product[b] | I stoichiometry[c] | conductivity, $\Omega^{-1}$ cm$^{-1}$ |
|---|---|---|---|
| 50 | 25.56 | 0.222 | |
| 100 | 36.75 | 0.376 | $3.4 \times 10^{-6}$ |
| 150 | 36.81 | 0.377 | |
| 200 | 39.61 | 0.424 | $1.3 \times 10^{-4}$ |
| 250 | 43.70 | 0.502 | $7.8 \times 10^{-3}$ |
| 300 | 46.30 | 0.558 | $1.5 \times 10^{-3}$ |
| 350 | 53.83 | 0.754 | |
| 400 | 52.98 | 0.729 | $1.2 \times 10^{-2}$ |
| 450 | 55.19 | 0.797 | 0.17 |
| 500 | 58.07 | 0.896 | |
| 1000 | 62.68 | 1.09 | 0.26 |
| 2500 | 77.16 | 2.19 | 1.29 |
| 5000 | 68.06 | 1.38 | $8.9 \times 10^{-2}$ |

[a] In each case reacted with 50.0 mg of polymer. [b] Result of the elemental analysis. [c] $y$ in the formula $(C_4H_6N_2I_y)_x$.

and Busch[6] (127–141 °C). Anal. Calcd for $C_8H_{16}N_6$: C, 48.96; H, 8.22; N, 42.82. Found: C, 48.79; H, 8.09; N, 42.64.

$C_{12}H_{22}N_8$. A solution of 3.00 g (0.026 mol) of $C_4H_{10}N_4$ dissolved in 50 mL of ethanol was brought to a gentle boil with vigorous stirring. To this was added dropwise (15 min) a solution of 1.2 mL (0.014 mol) of 2,3-butanedione dissolved in 20 mL of ethanol. This solution was boiled for an additional 15 min to reduce the volume and then refrigerated overnight. The yellow product was filtered and washed with cold ethanol and then cold ether: yield, 1.66 g (0.0060 mol), 46%; mp 140–147 °C with decomposition. Anal. Calcd for $C_{12}H_{12}N_8$: C, 51.78; H, 7.97; N, 40.26. Found: C, 51.64; H, 8.03; N, 40.12.

$C_{20}H_{34}N_{12}$. A solution of 1.00 g (5.1 mmol) of $C_8H_{16}N_6$ dissolved in 50 mL of ethanol was brought to a gentle boil with vigorous stirring. To this was added dropwise (15 min) a solution of 0.20 mL (2.3 mmol) of 2,3-butanedione dissolved in 20 mL of ethanol. This solution was boiled down to about 20 mL and then refrigerated overnight. The yellow product was filtered and washed with cold ethanol and then cold ether: yield, 0.44 g (0.99 mmol), 39%; mp 315–320 °C with decomposition. Anal. Calcd for $C_{20}H_{34}N_{12}$: C, 54.28; H, 7.74; N, 37.98. Found: C, 54.39; H, 7.67; N, 37.81.

$C_{28}H_{46}N_{16}$. $C_{12}H_{22}N_8$ (0.75 g, 2.7 mmol) and 1 drop of glacial acetic acid were added to 50 mL of ethanol and brought to a boil. To this was added dropwise (30 min) a solution of 0.12 (1.4 mmol) of 2,3-butanedione dissolved in 20 mL of ethanol. About halfway through the addition of the dione the solution turned cloudy. After all the dione had been added the solution was removed from the heat and precipitation occurred immediately. The solution was refrigerated overnight, and the yellow product was filtered and washed with cold ethanol and then with cold ether: yield, 0.32 g (0.53 mmol), 39%; mp 280–290 °C with decomposition. Anal. Calcd for $C_{28}H_{46}N_{16}$: C, 55.42; H, 7.64; N, 36.93. Found: C, 54.79; H, 7.69; N, 36.22.

$C_{44}H_{70}N_{24}$. $C_{20}H_{34}N_{12}$ (0.45 g, 1.0 mmol) and 1 drop of glacial acetic acid were added to 100 mL of ethanol and brought to a boil. To this was added dropwise (10 min) a solution of 0.04 mL (0.5 mmol) of 2,3-butanedione dissolved in 10 mL of ethanol. This solution was boiled an additional 5 min and then refrigerated overnight. The yellow product was filtered and washed with cold ethanol and then cold ether: yield, 0.38 g (0.41 mmol), 82%; mp 315–320 °C with decomposition. Anal. Calcd for $C_{44}H_{70}N_{24}$: C, 56.51; H, 7.54; N, 35.95. Found: C, 56.26; H, 7.41; N, 33.32.

$(C_4H_6N_2)_x$. To a 500-mL three-necked flask were added 6.92 g (0.061 mol) of $C_4H_{10}N_4$, 0.5 mL of glacial acetic acid, and 200 mL of DMSO. The solution was vigorously stirred and the temperature raised to 50 °C. To this was added dropwise (1 h) a solution of 4.0 mL (0.046 mol) of 2,3-butanedione dissolved in 25 mL of DMSO. The temperature of the solution was then raised to 100 °C and some of the water formed by the condensation reaction was distilled off. The stirred solution was maintained at 100 °C for 6 h. The flask was then cooled to 50 °C and a solution of 1.0 mL (0.011 mol) of 2,3-butanedione in 10 mL of DMSO was added over 30 min. The temperature was again brought to 100 °C and maintained for 18 h. The light brown product was filtered as the solution cooled and washed twice each with 10-mL portions of water, ethanol, acetonitrile, and finally ether. The product was dried under vacuum for 1 week: yield 3.19 g (0.039 mol based on the repeat unit), 34%; mp 310–320 °C with decomposition and with substantial pyrolysis of the polymer at about 300 °C. Anal. Calcd for $(C_4H_6N_2)_x$: C, 58.51; H, 7.37; N, 34.12. Found: C, 58.23; H, 7.31; N, 31.94.

**Table II.** Crystal, Data Collection, Data Reduction, and Refinement Details for the Crystal Structure of 2,3-Butanedione Dihydrazone

| | |
|---|---|
| formula | $C_4N_4H_{10}$ |
| formula wt, amu | 114.15 |
| temp, °C | 23 |
| space group | $P4_2/n$ (No. 86) (origin at $\bar{1}$ at $^1/_4$, $^1/_4$, $^1/_4$ from 4) |
| $a$, Å | 12.172 (4) |
| $c$, Å | 4.115 (1) |
| $V$, Å$^3$ | 609.7 (3) |
| $Z$ | 4 |
| density(calcd), g cm$^{-3}$ | 1.2435 (7) |
| density(obsd), g cm$^{-3}$ | 1.24 (1) |
| crystal dimens, mm | $0.25 \times 0.25 \times 0.45$ |
| crystal faces | {100}, {001} |
| crystal vol, mm$^3$ | 0.02812 |
| diffractometer | Syntex $P2_1$ |
| radiation | Mo K$\alpha$ (0.71073 Å) |
| monochromator | graphite crystal |
| scan type | $2\theta$–$\omega$ |
| scan speed, deg min$^{-1}$ Mo K$\alpha$ | 3.91 ($2\theta$) |
| background scan | crystal and detector held stationary at the beginning and end of the scan for a length of time equal to the scan time |
| scan width | 1.1° below K$\alpha_1$ to 1.1° above K$\alpha_2$ ($2\theta$) |
| $2\theta$ scan limits, deg | 3.0–65.0 |
| standard reflections | 3 every 97 reflections |
| indices | (112), ($\bar{1}$81), (811) |
| crystal stability | no indication of standard reflection decay during data collection |
| total reflections scanned | 2688 |
| unique reflections $I \geq 3\sigma(I)$ | 1195 |
| unique reflections $I \geq 0$ | 1964 |
| linear absorp coeff, cm$^{-1}$ | 1.104 |
| scattering factor source | international tables |
| parameters refined ($F$) | 57 |
| $R(F)$[a] | 0.077 |
| $R_w(F)$[a] | 0.057 |
| goodness of fit ($F$)[a] | 1.32 |
| $R(F)$[b] | 0.043 |
| $R_w(F)$[b] | 0.048 |
| goodness of fit ($F$)[b] | 1.43 |
| shift/esd | ≤0.01 |

[a] $F_o^2 \geq 0$. [b] $F_o^2 \geq 3\sigma(F_o^2)$.

**$I_2$ Doping of the Polymer.** Typically, 50.0 mg of the polymer was added to 100 mL of $CHCl_3$ in a 250-mL Erlenmeyer flask. To this was added a weighed amount of solid $I_2$; the flask was corked and the contents were stirred at room temperature for 24 h. This was vacuum filtered and rinsed with $CCl_4$ until the washings were clear of free $I_2$ and then air-dried. Generally, about 15% of the initial iodine reacted with polymer after 24 h. A series of experiments in which reaction time was varied was done, and it was found that the initial doping was very rapid; >50% of the doping occurred in the first 2 h and then the doping tailed off asymptotically toward the 24-h level. The results of the doping experiments are given in Table I.

**Instrumentation.** All IR spectra were run at room temperature as KBr pellets on a Perkin-Elmer 281B infrared spectrophotometer between 600 and 4000 cm$^{-1}$. Electrical conductivities were run on pressed pellets using the 4-probe Van der Pauw technique. Resistances were measured with an instrument built by Research Specialties, Chicago, IL; the system samples at a low ac frequency, 27 Hz, to minimize potential polarization problems associated with dc measurements, but with electronic circuitry designed to minimize capacitive effects.[7] Pellet thicknesses were measured with a calibrated reticle on a Bausch and Lomb Stereozoom 7 microscope. Because of variation in thickness across the pellet diameter, the error in the absolute conductivity measurement is estimated to be ±30%.

**X-ray Crystallography.** Recrystallization of 2,3-butanedione dihydrazone from 95% ethanol at 4 °C for 30 days yielded large ($0.5 \times 0.5 \times 1.0$ mm) crystals of tetragonal prismatic-pyramidal habit. The density of a single crystal was determined by flotation in $CCl_4$ diluted with $C_6H_{14}$. A crystal ($0.25 \times 0.25 \times 0.45$ mm) was cleaved from one of these larger crystals and mounted on a glass fiber with epoxy cement.

---

(6) Stratton, W. J.; Busch, D. H. *J. Am. Soc.* **1960**, *82*, 4834–4839.

(7) Phillips, T. E.; Anderson, J. R.; Schramm, C. J.; Hoffman, B. M. *Rev. Sci. Instrum.* **1979**, *50*, 263–265.

**Table III.** Final Positional and Thermal Parameters for All Atoms and Isotropic Thermal Parameters for the Hydrogens in the Asymmetric Unit of 2,3-Butanedione Dihydrazone[a]

| atom | $x/a$ | $y/b$ | $z/b$ | $U \times 10^2$ | $U_{11} \times 10^4$ | $U_{22} \times 10^4$ | $U_{33} \times 10^4$ | $U_{12} \times 10^4$ | $U_{13} \times 10^4$ | $U_{23} \times 10^4$ |
|---|---|---|---|---|---|---|---|---|---|---|
| N(1) | 0.6070 (6) | 0.0673 (6) | 0.2030 (2) | | 336 (4) | 299 (4) | 327 (4) | −48 (3) | 5 (3) | −17 (3) |
| N(2) | 0.6306 (7) | 0.1697 (6) | 0.3330 (2) | | 359 (4) | 345 (4) | 407 (5) | −62 (3) | −27 (4) | −71 (4) |
| C(1) | 0.4243 (8) | 0.1411 (9) | 0.0751 (3) | | 345 (5) | 357 (5) | 546 (7) | 17 (4) | −13 (5) | −70 (5) |
| C(2) | 0.5111 (7) | 0.0538 (7) | 0.0754 (2) | | 291 (4) | 297 (1) | 278 (4) | −34 (3) | 36 (4) | 11 (4) |
| H(1) | 0.573 (10) | 0.204 (10) | 0.417 (3) | 1.9 (3) | | | | | | |
| H(2) | 0.688 (10) | 0.161 (10) | 0.473 (3) | 2.4 (3) | | | | | | |
| H(3) | 0.457 (10) | 0.210 (10) | −0.008 (3) | 2.2 (3) | | | | | | |
| H(4) | 0.401 (11) | 0.159 (10) | 0.296 (4) | 3.2 (4) | | | | | | |
| H(5) | 0.3610 (10) | 0.119 (10) | −0.058 (3) | 3.5 (4) | | | | | | |

[a] The isotropic temperature factor is $\exp[-U \sin^2 \theta/8\lambda^2\pi^2]$, where $U = B/8\pi^2$. The complete anisotropic temperature factor is $\exp[-2\pi^2(U_{11}h^2a^{*2} + U_{22}k^2b^{*2} + U_{33}l^2c^{*2} + 2U_{12}hka^*b^* + 2U_{13}hla^*c^* + 2U_{23}klb^*c^*)]$.

This crystal was aligned on a Syntex P2$_1$ diffractometer. The unit cell was determined from the least-squares refinement of 15 independent reflections with 20.0° ≤ 2$\theta$ ≤ 30.0°. Intensity data were collected at room temperature from 3.0° ≤ 2$\theta$ ≤ 65.0°. The intensity of three check reflections did not change appreciably over the course of data collection. Crystal data and data collection details are found in Table II.

## Results and Discussion

**Synthesis.** 2,3-Butanedione dihydrazone ($x = 1$) was synthesized by using a variation of the procedure of Busch and Bailar,[5] and butanedione dihydrazone azine ($x = 2$) was prepared as described by Stratton and Busch,[6] Higher oligomers were synthesized by refluxing a 2:1 mole ratio of the appropriate hydrazone azine with 2,3-butanedione in ethanol, with acetic acid as a catalyst,

$$2H_2N\text{-}[N{=}C(CH_3){-}C(CH_3){=}N]_x\text{-}NH_2 + CH_3OCCOCH_3 \xrightarrow[H^+]{EtOH} H_2N\text{-}[N{=}C(CH_3){-}C(CH_3){=}N]_{2x+1}\text{-}NH_2 + 2H_2O$$

This method works for product oligomers up to $x = 5$. Long-chain polymers have been prepared previously,[8] but we have found that a more uniform molecular weight distribution of products can be obtained by reacting equimolar quantities of 2,3-butanedione dihydrazone with 2,3-butanedione in DMSO and distilling off the water coproduct. The higher molecular weight oligomers and polymers are yellow to brown powders, are insoluble in all common solvents, are stable to air, have high melting points (>300 °C for the longest chain polymers), and are surprisingly stable toward hydrolysis—there was no evidence of decomposition even after prolonged refluxing of the polymer in water.

The highest molecular weight oligomers and polymers all give low analyses for nitrogen. This is most reasonably accounted for if a portion of the end groups are ketone fragments rather than hydrazone, an assumption supported by the IR spectra (vide infra). Unfortunately, this complicates the estimation of the polymer molecular weight by use of the elemental analysis. If it is assumed that all the end groups are ketone, then the observed carbon to nitrogen ratio of 2.1 indicates a chain length of $x = 20$ monomer units (MW = 1600); if it is assumed that the end groups are all hydrazone, then the carbon analysis alone gives a chain length of $x = 80$ monomers (MW = 6500). Thus, the elemental analysis gives reasonable boundaries for the molecular weight but cannot give a better estimate of the chain length since the relative amounts of ketone and hydrazone end groups are unknown. Because of the polymer's limited solubility, estimation of the molecular weight by chromatographic or light scattering techniques is not possible. However, analysis of the IR spectra (vide infra) indicates $x \geq 45$ (MW = 3700), in agreement with the elemental analysis.

The polymer can be doped by iodine by stirring a slurry of the polymer with a chloroform solution of the dopant. A large excess of iodine is required to achieve any given level of iodine uptake, indicating that the charge-transfer reaction has a fairly small equilibrium constant. The doped materials do not melt even after losing iodine, up to 320 °C, although the pristine polymers do melt in this range. The ionic form of the iodine in the doped materials is unknown.

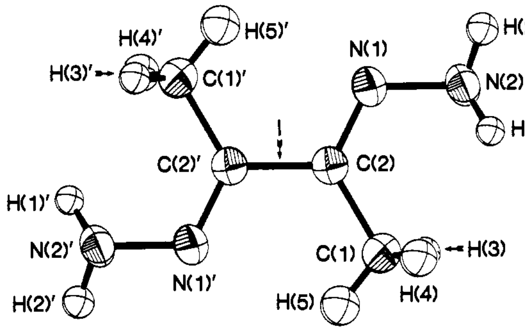

**Figure 1.** ORTEP labeling diagram for 2,3-butanedione dihydrazone. The thermal ellipsoids are drawn at the 50% probability level. Note the center of inversion between C(2) and C(2)'.

**Table IV.** Bond Lengths (Å) for All Atoms in 2,3-Butanedione Dihydrazone

| from | to | dist | from | to | dist |
|---|---|---|---|---|---|
| N(1) | N(2) | 1.387 (1) | N(2) | H(1) | 0.888 (12) |
| N(1) | C(2) | 1.291 (1) | N(2) | H(2) | 0.911 (13) |
| C(1) | C(2) | 1.498 (1) | C(1) | H(3) | 0.985 (13) |
| C(2) | C(2) | 1.474 (2) | C(1) | H(4) | 0.973 (15) |
| | | | C(1) | H(5) | 0.985 (13) |

**X-ray Crystallography.** The systematic absences ($0k0$, $k = 2n + 1$, $h0l$, $h + 1 = 2n + 1$) and the $4/m$ Laue symmetry observed were consistent with the space group $P4_2/n$.[9] The positions of the carbon and nitrogen atoms were determined by direct methods in the space group $P4_2/n$.[9] After several cycles of least-squares refinement a difference Fourier map revealed the positions of the five hydrogens of the asymmetric unit. The carbon and nitrogen atoms were refined anisotropically and the hydrogen atoms were refined isotropically, with the data $I \geq 3\sigma(I)$ resulting in a data to parameter ratio of 21:1. Refinement to convergence resulted in the final agreement factors $R(F) = 0.043$ and $R_w(F) = 0.048$. Structure solution and refinement details are given in Table II. The final positional and thermal parameters are given in Table III.

2,3-Butanedione dihydrazone crystallizes in the $E$ conformation with a crystallographically imposed center of inversion in the bond between C(2) and C(2)' (Figure 1). Bond lengths are given in Table IV. The C(2)–C(2)' single bond (1.474 (2) Å) is short in comparison with the normal aliphatic C–C bond length of 1.54 Å while it is within the range of C–C bond lengths (1.462 (20)–1.483 (15) Å) observed in the related compounds 2,3-butanedione bis(2'-nitrophenylhydrazone)[10a] (**1**), ($E$,$E$)-2,3-buta-

---

[8] (a) Zimmerman, B. G.; Lochte, H. L. *J. Am. Chem. Soc.* **1936**, *58*, 948–949. (b) Karpacheva, G. P. *Russ. J. Phys. Chem.* (*Engl. Transl.*) **1965**, *39*, 1609–1611.

[9] The UCLA Crystallographic Computing Package, Jan 5, 1982.

[10] (a) Edwards, J. W.; Hamilton, W. C. *Acta Crystallogr., Sect. B* **1972**, *28*, 1362–1366. (b) Willey, g. R.; Drew, M. G. B. *Acta Crystallogr., Sect. C* **1983**, *39*, 403–407. (c) Willey, G. R.; Drew, M. G. B. *Acta Crystallogr., Sect. C* **1985**, *41*, 589–594. These structures were the only ones found by searching the Cambridge Structural Database for the fragment —NH—N=C(CH$_3$)—C(CH$_3$)=N—NH—.

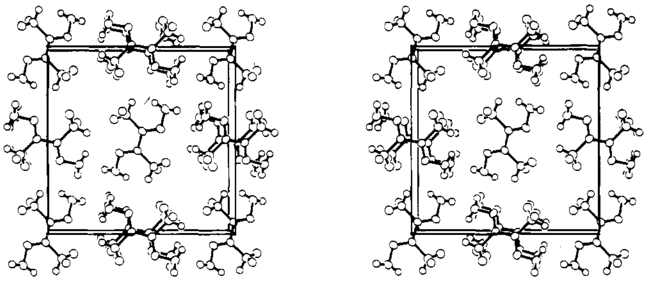

**Figure 2.** ORTEP packing diagram of 2,3-butanedione dihydrazone. The thermal ellipsoids are drawn at the 50% probability level. The *c* axis is perpendicular to the page, and the *b* axis points to the right.

nedione bis(4′-nitrophenylhydrazone)[10b] (**2**), and dimethylglyoxal bisguanylhydrazone[10c] (**3**). The bond length between C(1) and C(2) (1.498 (1) Å) is within the range of comparable bond lengths (1.480 (11)–1.503 (2) Å) observed for **1**, **2**, and **3**. Similarly, the C–N bond length (1.291 (1) Å) falls in the range observed (1.282 (12)–1.306 (10) Å) for **1**, **2**, and **3**. The N–N bond length (1.387 (1) Å) is longer than the those found in **1**, **2**, and **3** (1.356 (2)–1.371 (8) Å). A likely explanation is as follows: in 2,3-butanedione dihydrazone the amine nitrogens terminate the molecular chain while in **1**, **2**, and **3** the amine nitrogens are an internal part of the extended $\pi$ system; the effect of the conjugated $\pi$ system on bond lengths will be larger in the center of the chain than at the termini. The mean C–H bond length in 2,3-butanedione dihydrazone is 0.981 (7) Å and the mean N–H bond length is 0.900 (16) Å.[11] In compound **3** the C–H and N–H bond lengths are 0.935 (8) and 0.903 (21) Å, respectively. Table V contains the bond angles for 2,3-butanedione dihydrazone along with ranges for the comparable angles of **1**, **2**, and **3**.

The molecules of 2,3-butanedione dihydrazone are planar with a root-mean-square deviation from the least-squares plane of 0.02 Å. The values of the deviations of each nonhydrogen off the least-squares plane of the molecule are ±0.025 (1) Å for N(1) and N(1)′, ±0.018 (1) Å for N(2) and N(2)′, ±0.006 (1) Å for C(1) and C(1)′, and ±0.009 (1) Å for C(2) and C(2)′. This planarity is probably due to some double-bond character in the C(2)–C(2)′ bond (vide supra). Planarity is also observed for **1**, **2**, and **3**.

Analysis of the molecular packing indicates that there may be some weak intermolecular hydrogen bonding between molecules related by the $4_2$ axis; that is, each hydrogen bond has a component along the *a* or *b* axis and a component along the *c* axis (Figure 2). The shortest interaction of this type is N(2)–H(2)–N(2) where the intermolecular N(2)–H(2) distance is 2.31 (1) Å and the angle about the hydrogen is 177 (1)°. These are typical values of hydrogen bond lengths and angles.[12] There are also a number of intermolecular nitrogen contacts without bridging hydrogens. The shortest of these is between N(1) and N(2) at 3.209 (1) Å. Both intramolecular hydrogen bonding and intermolecular hydrogen bonding are observed in **1**, **2**, and **3**. However, the hydrogen bonding occurs between the amine nitrogen and a nonnitrogen atom, so a direct comparison is not possible. The intermolecular hydrogen bonding observed in 2,3-butanedione dihydrazone indicates that this compound may exhibit proton conductivity,[13] a possibility that is currently under investigation.

**IR Spectroscopy.** The IR spectra of a series of polyazines with sequentially increasing chain length are shown in Figure 3A–E. The spectrum of 2,3-butanedione dihydrazone matches that previously reported:[14] the peaks at 3325 (N–H antisymmetric stretch), 3185 (N–H symmetric stretch), 1630 ($NH_2$ internal deformation), and 735 cm$^{-1}$ (N–H rocking) are all N–H vibrations that shift upon deuteriation. Bands at 1305, 1275, 1078, and 935 cm$^{-1}$ are also diminished by exchange with $D_2O$ and thus, although not assigned, must have substantial N–H character in them (although they probably are not pure N–H vibrations). Absorptions at 3000 (C–H antisymmetric stretch), 2900 (C–H symmetric stretch), 1560 (C=N stretch), 1440 (C–$CH_3$ antisymmetric deformation), 1355 (C–$CH_3$ symmetric deformation), and 1120 cm$^{-1}$ (N–N stretch) are unaffected by deuteriation. As shown by the crystal structure, these vibrations correspond to a molecule with the double bonds in the *E* conformation ($NH_2$ and $CCH_3$ trans), the C–C bond in the anti conformation (methyl groups trans), and the N–N bond in the gauche conformation (lone pairs at a 90° angle to the $\pi$ system). The lower energy than usual C=N stretch is consistent with conjugation of the $\pi$ system along the chain, in accordance with the X-ray results.

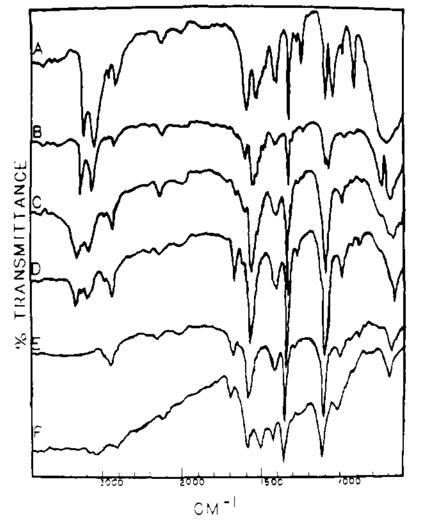

**Figure 3.** IR spectra of various chain length polyazines: (A) $H_2N$–$[C_4H_6N_2]$–$NH_2$ (2,3-butanedione dihydrazone); (B) $H_2N$–$[C_4H_6N_2]_2$–$NH_2$; (C) $H_2$–$[C_4H_6N_2]_4$–$NH_2$; (D) $H_2N$–$[C_4H_6N_2]_{11}$–$NH_2$; (E) –$[C_4H_6N_2]_x$–; (F) –$[C_4H_6N_2I_{0.57}]_x$–. All spectra were taken as KBr pellets; the peak at about 2300 cm$^{-1}$ is due to an impurity in the KBr.

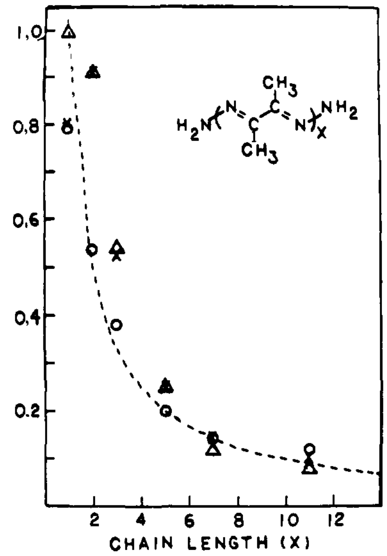

**Figure 4.** Plot of the intensity ratio *I*(N–H)/*I*(1355 cm$^{-1}$) for the 1630- (○), 3180- (△), and 3370-cm$^{-1}$ (×) IR bands vs. chain length. The dashed line is the function *I*(N–H)/*I*(1355 cm$^{-1}$) = 1/*x*.

The intensity of the N–H vibrational bands steadily decreases as oligomer size increases since the $NH_2$ groups only exist at polyazine chain ends. In fact, the intensities of the N–H bands serve as good semiquantitative guides to the chain length of the polymer. Using the very strong, narrow, and invariant band at

---

[11] Hydrogen bond lengths determined by X-ray crystallography are shortened relative to their actual values: (a) Hamilton, W. C.; Ibers, J. A. In *Hydrogen Bonding in Solids*; W. A. Benjamin: New York, 1968. (b) Churchill, M. R. *Inorg. Chem.* **1973**, *12*, 1213–1214.

[12] Cotton, F. A.; Wilkinson, G. *Advanced Inorganic Chemistry*, 4th ed.; Wiley-Interscience: New York, 1980; pp 219–224.

[13] (a) Loehlin, J. H. *Acta Crystallogr., Sect. C: Cryst. Struct. Commun.* **1985**, *C41*, 210–212. (b) Glasser, L. *Chem. Rev.* **1975**, *75*, 21–65.

[14] Stoufer, R. C.; Busch, D. H. *J. Am. Chem. Soc.* **1960**, *82*, 3491–3495.

Table V. Bond Angles (Deg) for All Atoms in 2,3-Butanedione Dihydrazone and Compounds **1**, **2**, and **3**[a]

| from | through | to | angle | range obsd for $-NHN{=}C(CH_3)C(CH_3){=}NNH-$ |
|---|---|---|---|---|
| N(2) | N(1) | C(2) | 117.29 (8) | 117.11 (13)–117.4 (10) |
| N(1) | N(2) | H(1) | 114.3 (7) | 126.6 (1.1)[b] |
| N(1) | N(2) | H(2) | 107.4 (8) | na |
| H(1) | N(2) | H(2) | 114.4 (10) | na |
| C(2) | C(1) | H(3) | 108.7 (6) | 109.8 (2.2)[b] |
| C(2) | C(1) | H(4) | 111.0 (8) | 109.8 (2.2)[b] |
| C(2) | C(1) | H(5) | H(5) | 109.8 (2.2)[b] |
| H(3) | C(1) | H(4) | H(4) | 109.8 (2.2)[b] |
| H(3) | C(1) | H(5) | 110.4 (10) | 109.8 (2.2)[b] |
| H(4) | C(1) | H(5) | 110.6 (11) | 109.8 (2.2)[b] |
| N(1) | C(2) | C(2) | 116.70 (9) | 112.9 (7)–115.7 (10) |
| N(1) | C(2) | C(1) | 123.20 (8) | 123.9 (9)–124.9 (7) |
| C(1) | C(2) | C(2) | 120.09 (10) | 120.4 (9)–122.2 (7) |

[a] Reference 3. [b] Reference 3c only.

1355 cm$^{-1}$ as an internal reference allows us to plot the ratio $I$(N–H)/$I$(1355 cm$^{-1}$) vs. chain length (Figure 4). The ratio of the number of N–H bonds to the number of C–CH$_3$ bonds in a polyazine is $2/x$, and $I$(N–H)/$I$(1355 cm$^{-1}$) should be proportional to this. The 1630-, 3185-, and 3325-cm$^{-1}$ bands all fit very nicely to the function $1/x$, plotted as the dashed line in Figure 4, although it is a bit surprising that all three bands have the same proportionality constant (which indicates that these three bands all have about the same molar absorptivity). In the longest chain polymer the IR spectrum shows no trace of any N–H band (Figure 3E; the band at 1690 cm$^{-1}$ is due to residual ketone fragments); if the limit of detectability above the background is 3% $T$ (a conservative estimate: the C–H bands in Figure 3E are 8% $T$ above background), then extrapolating the function $1/x$ from Figure 4 gives a chain length of $x = 45$, or a molecular weight of about 3700.

It also must be noted that the position and band shape of the C–CH$_3$ (1440, 1355 cm$^{-1}$) and C=N (1560 cm$^{-1}$) bands are unaffected by chain length. This strongly indicates that the conformations about these bonds are the same in short-chain and long-chain materials. Thus we believe that these polymers are planar with the double bonds in the $E$ (chain atoms trans) conformation and the single bonds in the anti conformation. This conformation is the most stable for both steric and electronic reasons: the repulsion between methyl groups is alleviated and yet the $\pi$ bonds are conjugated and can be delocalized, at least to a small degree.

The IR spectrum of a typical doped polyazine, $-[C_4H_6N_2I_{0.57}]_x-$, is shown in Figure 3F. In the fingerprint region below 1800 cm$^{-1}$ the spectra of doped and undoped polymers are essentially the same, indicating that the structural integrity of the chain is retained upon doping. However, iodine doping induces two new features to the polyazine spectrum: one band at or above 4000 cm$^{-1}$ and another band at 1505 cm$^{-1}$. The narrow, lower energy band at 1505 cm$^{-1}$ is reminiscent of the doping-induced absorption in polyacetylene[15] at 1370 cm$^{-1}$ since it grows in intensity with increased doping levels and is probably associated with a partially oxidized double bond. The higher energy band near 4000 cm$^{-1}$ is very broad and intense and may be of electronic origin and is probably the free-electron absorption typically seen in conducting polymers. Further spectroscopic studies are being undertaken to better understand the nature of these bands.

Spectra in the UV–vis region were also measured for samples dispersed in KBr pellets. Undoped polyazine has a peak at 340 nm that tails into the visible, accounting for the yellow color of this material. As iodine is doped into the polyazine, the polymer grows progressively darker and the electronic spectra show increasing absorption over the entire visible region, with no observable peaks or structure seen. Very heavily iodine-doped polyazines ($y > 1.3$) are black. The lack of defined structure in the absorption spectra makes interpretation fruitless; we are currently trying to find ways to obtain more useful spectra.

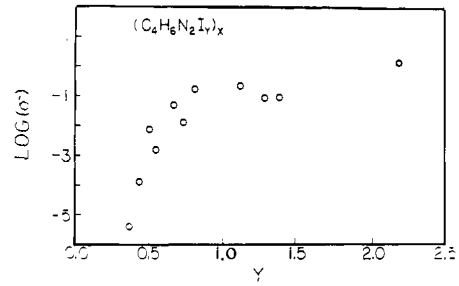

**Figure 5.** Room-temperature electrical conductivity ($\Omega^{-1}$ cm$^{-1}$) of iodine-doped polyazines as a function of dopant stoichiometry.

**Electrical Conductivity.** As predicted by our extended-Hückel calculations,[3] pristine polyazine polymers are poor conductors, $\sigma < 10^{-6}$ $\Omega^{-1}$ cm$^{-1}$. However, we have been able to significantly increase the conductivity by iodine doping. The room-temperature conductivity on pressed pellets varies substantially with dopant level; for $[C_4H_6N_2I_y]_x$ we have been able to vary $y$ from 0 to 2.2, with the room-temperature conductivities monotonically increasing to as high as 1.3 $\Omega^{-1}$ cm$^{-1}$ (Figure 5). Because the form of the iodine is not determined by the elemental analysis or the IR spectra, the amount of charge transferred from the polymeric donor to the acceptor is not known. The conductivity vs. dopant concentration plot suggests that an insulator–semiconductor transition occurs at about $y = 0.4$ and the conductivity levels out at about $y = 1.0$, although iodine uptake continues. Unfortunately, we have been unable to measure conductivities for samples with less iodine than shown in Figure 5. A detailed investigation of the temperature dependences of the conductivities of these doped polyazines is in progress.

## Conclusion

We have described the preparation and characterization of a series of air-stable monomeric, oligomeric, and polymeric azine materials. The crystal structure of the monomer, 2,3-butanedione dihydrazone, was determined, and this molecule was found to be planar with short single bonds and long double bonds and with all bonds in the trans (or anti) conformation. The correlation of the IR spectra of the monomer with those of the increasingly higher molecular weight oligomers showed that this structural motif was retained up to the longest chain polymers synthesized. Thus, structurally, polyazine is similar to *trans*-polyacetylene. Unlike polyacetylene, we have not found a cis analogue, probably due to the steric repulsion of the pendant methyl groups along the polymer chain. End-group analysis of the polymer by IR spectroscopy indicated a molecular weight of at least 3700.

Polyazine can be reacted with iodine to give electrically conducting materials. The IR spectra of doped polymers showed that the structural integrity of the chain is retained upon exposure to I$_2$; in addition, two new absorptions appear that, as yet, have not been identified. The electrical conductivity of iodine-doped polyazine can reach as high as 1.3 $\Omega^{-1}$ cm$^{-1}$ at room temperature.

---

(15) Fincher, C. R., Jr.; Ozaki, M.; Heeger, A. J.; MacDiarmid, A. G. *Phys. Rev. B* **1979**, *19*, 4140–4148.

*J. Am. Chem. Soc.* **1987**, *109*, 5765-5780 5765

Further spectroscopic and conductivity studies are in progress to elucidate the mechanism of charge transport in these materials.

**Acknowledgment** is made to the donors of the Petroleum Research Fund, administered by the American Chemical Society, and Research Corp. for partial support of this work. J.D.F, thanks B. F, Goodrich Co. for financial support through a B. F. Goodrich Fellowship at CWRU.

**Supplementary Material Available**: Table of structure factors for 2,3-butanedione dihydrazone (9 pages). Ordering information is given on any current masthead page.

---

# Catalytic Asymmetric Epoxidation and Kinetic Resolution: Modified Procedures Including in Situ Derivatization†

**Yun Gao, Robert M. Hanson, Janice M. Klunder, Soo Y. Ko, Hiroko Masamune, and K. Barry Sharpless***

*Contribution from the Department of Chemistry, Massachusetts Institute of Technology, Cambridge, Massachusetts 02139.* *Received July 11, 1986*

**Abstract**: The use of 3A or 4A molecular sieves (zeolites) substantially increases the scope of the titanium(IV)-catalyzed asymmetric epoxidation of primary allylic alcohols. Whereas without molecular sieves epoxidations employing only 5 to 10 mol % Ti(O-*i*-Pr)$_4$ generally lead to low conversion or low enantioselectivity, in the presence of molecular sieves such reactions generally lead to high conversion (>95%) and high enantioselectivity (90–95% ee). The epoxidations of 20 primary allylic alcohols are described. Especially noteworthy are the epoxidations of cinnamyl alcohol, 2-tetradecyl-2-propen-1-ol, allyl alcohol, and crotyl alcohol—compounds which heretofore had been considered difficult substrates for asymmetric epoxidation. In the case of allyl alcohol, the use of cumene hydroperoxide substantially increases both the reaction rate and the conversion, even in the absence of molecular sieves. In general, enantioselectivities are slightly depressed (by 1–5% ee) relative to reactions employing 50–100 mol % Ti(O-*i*-Pr)$_4$. The epoxidation of low molecular weight allylic alcohols is especially facilitated and, in conjunction with in situ derivatization, provides for the synthesis of many epoxy alcohol synthons which were previously difficult to obtain. The kinetic resolution of four secondary allylic alcohols with 10 mol % Ti(O-*i*-Pr)$_4$ is also described. The role of molecular sieves in the reaction and the effects of variation in reaction stoichiometry, oxidant, and tartrate are discussed.

The reaction of an allylic alcohol with *tert*-butyl hydroperoxide (TBHP) in the presence of Ti(O-*i*-Pr)$_4$ and diethyl tartrate (DET) to form an epoxy alcohol of high enantiomeric purity was introduced in 1980 (Scheme I).[1] Since then, much has been learned about this asymmetric epoxidation process, Several reviews have been published,[2] and two theses from these laboratories have dealt with mechanistic aspects of the reaction.[3,4]

The epoxidation as initially described employs a stoichiometric amount of catalyst, even though, as noted in one of the footnotes to the original report, reactions of certain substrates can be carried out with as little as 10% catalyst with little loss of enantioselectivity and some increase in yield.

In 1981, we reported that, with slight modifications, the same procedure also effects the kinetic resolution of secondary allylic alcohols (Scheme II).[5] Again, it was noted that for certain substrates just 0.25 equiv of catalyst can be effective,

Over the next 4 years, no major modifications to the procedure were introduced. The asymmetric epoxidation reaction has proven to have wide applicability, even with use of a stoichiometric amount of catalyst, and has been the subject of an *Organic Syntheses* preparation.[6]

We recently reported a simple modification of the original procedure which allows the asymmetric epoxidation to be carried out with just 5–10% catalyst.[7] The key feature of the catalytic modification is the use of molecular sieves (zeolites). We now report in full our studies relating to this new procedure. The modifications presented here significantly expand the scope, effectiveness, convenience, and economy of the reaction. In the first part of this report, we present results relating to the synthesis of epoxy alcohols and their in situ derivatization, as well as kinetic resolutions involving catalytic amounts of the titanium–tartrate complex. In the second part we discuss factors which influence the reaction.

**Scheme I**

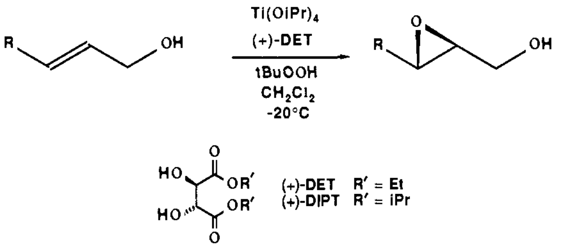

**Scheme II**

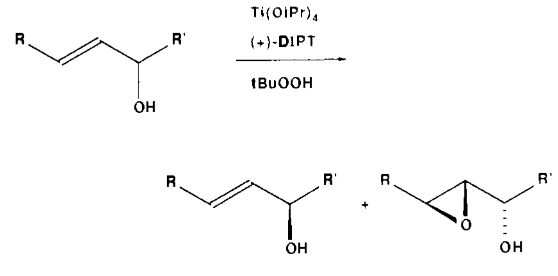

---

† Dedicated to Professor George Büchi on the occasion of his 65th birthday.

(1) Katsuki, T.; Sharpless, K. B. *J. Am. Chem. Soc.* **1980**, *102*, 5974.

(2) Finn, M. G.; Sharpless, K. B. In *Asymmetric Synthesis*; Morrison, J. D., Ed.; Academic Press: New York, 1985; Vol. 5, Chapter 8, 247. Rossiter, B. E. In *Asymmetric Synthesis*; Morrison, J. D., Ed.; Academic Press: New York, 1985; Vol. 5, Chapter 7, 193. Pfenninger, A. *Synthesis* **1986**, 89–116. The last of these reviews (Pfenninger) is somewhat out of date even for the stoichiometric reaction, especially with respect to the best experimental procedures and catalyst structure; the *Asymmetric Synthesis* reviews are more current.

0002-7863/87/1509-5765$01.50/0